

# Node Similarity Within Subgraphs of Protein Interaction Networks

Orion Penner,<sup>1</sup> Vishal Sood,<sup>1,2</sup> Gabriel Musso,<sup>3</sup> Kim Baskerville,<sup>4</sup> Peter Grassberger,<sup>1,2</sup> and Maya Paczusi<sup>1</sup>

<sup>1</sup>*Complexity Science Group, University of Calgary, Calgary, Alberta T2N 1N4, Canada*

<sup>2</sup>*Institute for Biocomplexity and Informatics, University of Calgary, Calgary, Alberta T2N 1N4, Canada*

<sup>3</sup>*Department of Medical Genetics and Microbiology,*

*University of Toronto, Toronto, Ontario M5S 3E1, Canada*

<sup>4</sup>*Perimeter Institute for Theoretical Physics, Waterloo, Ontario N2L 2Y5, Canada*

(Dated: November 13, 2018)

We propose a biologically motivated quantity, *twinness*, to evaluate local similarity between nodes in a network. The twinness of a pair of nodes is the number of connected, labeled subgraphs of size  $n$  in which the two nodes possess identical neighbours. The graph animal algorithm is used to estimate twinness for each pair of nodes (for subgraph sizes  $n = 4$  to  $n = 12$ ) in four different protein interaction networks (PINs). These include an *Escherichia coli* PIN and three *Saccharomyces cerevisiae* PINs – each obtained using state-of-the-art high throughput methods. In almost all cases, the average twinness of node pairs is vastly higher than expected from a null model obtained by switching links. For all  $n$ , we observe a difference in the ratio of type **A** twins (which are *unlinked* pairs) to type **B** twins (which are *linked* pairs) distinguishing the prokaryote *E. coli* from the eukaryote *S. cerevisiae*. Interaction similarity is expected due to gene duplication, and whole genome duplication paralogues in *S. cerevisiae* have been reported to co-cluster into the same complexes. Indeed, we find that these paralogous proteins are over-represented as twins compared to pairs chosen at random. These results indicate that twinness can detect ancestral relationships from currently available PIN data.

PACS numbers: 87.14.Ee, 02.70.Uu, 87.10.+e, 89.75.Fb, 89.75.Hc

## I. INTRODUCTION

Proteins constitute the machinery that carry out cellular processes by forming stable or transitory complexes with each other – organized perhaps into a web of overlapping modules. Information about this complex system can be condensed into a protein interaction network (PIN), which is a graph where nodes are proteins and links are measured or inferred pairwise binding interactions in a cell. Major efforts over the years devoted to resolving protein interactions have employed both small-scale and large-scale techniques. High throughput methods, such as yeast two hybrid (Y2H) and tandem affinity purification (TAP) have recently generated vast amounts of protein interaction data [1, 2, 3], allowing PINs from different organisms, experiments, research teams etc. to be compared.

A basic statistical feature of any network is its degree distribution,  $P(k)$ , for the number of links,  $k$ , connected to a node. In this respect, a variety of networks have been shown [4] to deviate decisively from a random graph, where the degree distribution is Poisson. In fact, early work suggested that degree distributions for PINs were power-law or scale-free [5]. However, as demonstrated in Fig. 1, degree distributions for recently obtained PINs are neither power-law nor particularly stable across different state-of-the-art constructions for the same organism – here the budding yeast *S. cerevisiae*. Note that all of the data sets studied here are based on the TAP-MS technique, except for Batada *et al.*, which is a compilation of data obtained from a number of different techniques.

Despite the empirical inconsistency presented by PIN degree distributions, similar local structures can stand out when each network is compared to a null model where links are switched while retaining the original degree sequence [6, 7]. Subgraphs that are significantly over-abundant are referred to as motifs, while subgraphs that are significantly under-represented are referred to as anti-motifs [6]. It has been reported that proteins within motifs are more conserved than other proteins [8]. In PINs, dense subgraphs containing 3 or 4 nodes are motifs, while tree-like subgraphs are anti-motifs [9].

Complementary to the search for motifs, graph clustering algorithms have been applied to identify components or complexes in PINs. By construction, these components tend to contain a high density of links but are weakly connected to the rest of the network (see e.g. Refs. [10, 11]). Complexes identified in this manner can contain up to 100 or more proteins, with on-going debate [11] as to their biological significance. However, biological processes such as signal transduction, cell-fate regulation, transcription, and translation typically involve a few tens of proteins. In previous work [10] mesoscale (5-25) protein clusters have also been identified using graph clustering algorithms. These clusters were matched with groups of proteins known to form complex macromolecular structures, or modules of proteins that participate in a specific function in the cell [10].

The subgraphs we probe lie within the mesoscale range, but our technique avoids using clustering methods to identify components. Rather we directly estimate frequencies of occurrence of connected subgraphs of different sizes

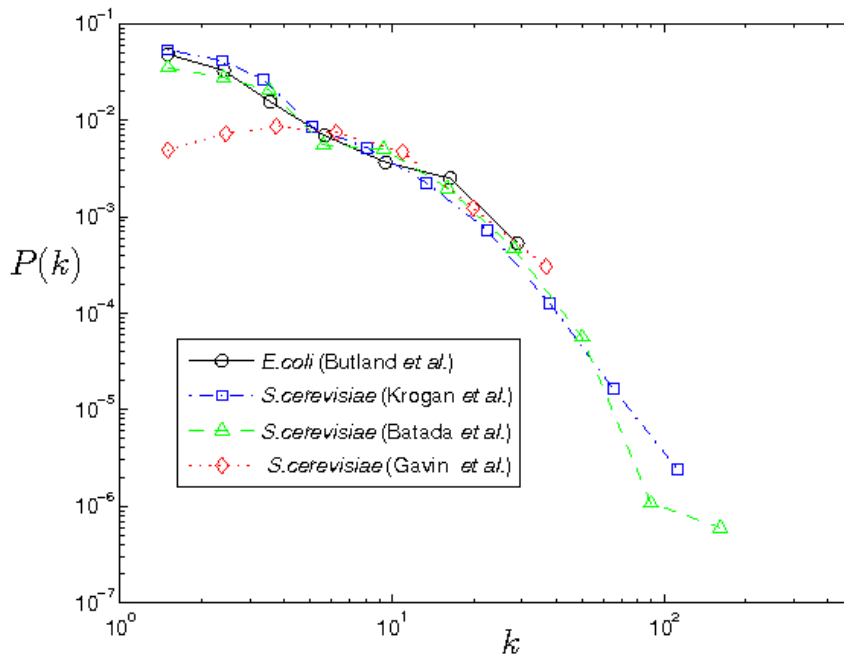


FIG. 1: Degree distribution  $P(k)$  as a function of degree  $k$  for four different PINs. Note the systematic curvature and the variation between different data sets for the budding yeast *S. cerevisiae*.

and analyze properties of these subgraph collections in the network. The particular properties we focus on here involve node similarity within subgraphs, quantified through a measure we refer to as 'twinness'.

Just as degree distributions are not consistent across currently available PINs, extensive studies of subgraph counts [9] as well as modular structures [11] show discrepancies among PINs nominally representing the same organism (again *S. cerevisiae*). Hence, in cases where the results are not demonstrably robust over current data sets, one can expect conclusions based on these results to change as the methods to construct PINs improve. On the other hand, statistical measurements that are relatively consistent over different PINs for the same organism can *a priori* be considered more robust. This is the criteria we use to decide whether or not results from our analyses are reliable.

A dominant feature of biological evolution affecting the structure of PINs is gene duplication, either of e.g. a single gene or in rare cases the whole genome, followed by divergence of the duplicates through mutation and selection. A pair of genes that evolved from the same ancestral gene is termed a paralogous gene pair, and the two proteins coded by such a gene pair are referred to as a paralogous protein pair. Remarkably, the whole genome of the yeast *S. cerevisiae* is believed to have duplicated approximately 100 million years ago [12]. Evolution ensuing duplication can silence duplicates. In fact, only about 10% of the duplicated genes are known to have been retained in *S. cerevisiae*. Obviously, just after a duplication event, paralogous proteins interact with exactly the same set of proteins. However, evolution following the duplication event results in loss of some shared interactions, or gain of new interactions by one of the two paralogous proteins. Divergence following duplication thus reduces interaction similarity of paralogues. Early studies of paralogues in the yeast PIN showed little or no interaction similarity [13]. However, when paralogues resulting from the whole genome duplication event (WGD) in *S. cerevisiae* were studied separately, those paralogues were much more likely than randomly chosen pairs to share at least one neighbour [14, 15], and were significantly more likely to be co-clustered within the same protein complex. This suggests that in connected subgraphs much smaller than the entire network WGD paralogues may be observed to have the same neighbours. Indeed, our findings reliably confirm this hypothesis.

### A. Summary

In Section II, we define twinness as a measure of node similarity within local structures in networks, summarize the graph animal algorithm used to estimate twinness, the Monte Carlo procedure used to construct null models, and the experimental methods through which the different PINs [1, 2, 3] we analyze were constructed. In Section III, we

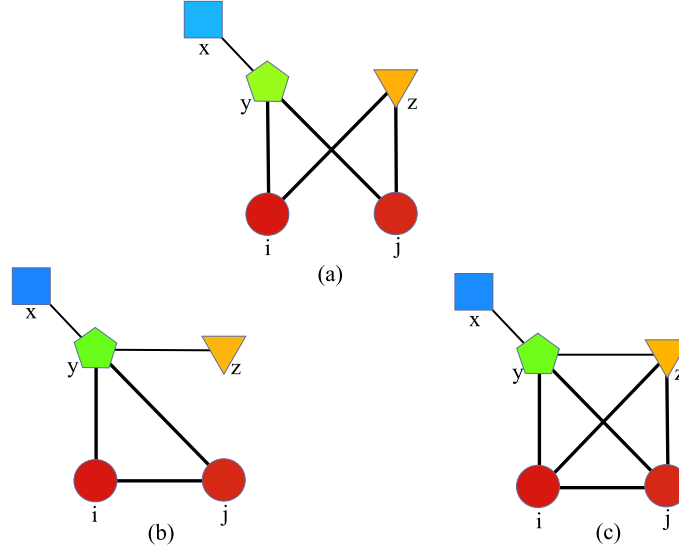


FIG. 2: Examples of twins in a connected, labeled subgraph of size  $n = 5$ . Nodes  $i$  and  $j$  are twins. (a) Type **A** twins: defined as those satisfying  $A_{il} = A_{jl} \quad \forall l \in \mathcal{H}$  and  $k_i^{\mathcal{H}}, k_j^{\mathcal{H}} \geq 2$ . (b) Type **B** twins: defined as those satisfying  $A_{il} = A_{jl} \quad l \neq i, j \quad \forall l \in \mathcal{H}$  with  $k_i^{\mathcal{H}}, k_j^{\mathcal{H}} \geq 2$  and  $A_{ij} = 1$ . (c) Type **B'** twins: defined as those satisfying  $A_{il} = A_{jl} \quad l \neq i, j \quad \forall l \in \mathcal{H}$  and  $k_i^{\mathcal{H}}, k_j^{\mathcal{H}} \geq 3$  and  $A_{ij} = 1$ . All type **B'** twins are also type **B** twins.

present our results. We measure twinning in connected, labeled subgraphs of size  $n$  in *E. coli* and *S. cerevisiae* PINs. These are uniformly sampled using the graph animal algorithm [9]. For each subgraph, pairs of nodes that share identical subgraph neighbourhoods are identified. Twins are divided into two types depending on whether (type **B**) or not (type **A**) they are linked to each other. For all PINs and for  $n = 4$  to  $n = 12$  twinning is (almost always) significantly higher than expected from the null hypothesis. Our consistent observation for twinning for three different *S. cerevisiae* PINs speaks to its robustness as a structural feature of PINs. Also, type **A** twinning is dominant for the prokaryote *E. coli*, while type **B** twinning is dominant for eukaryote *S. cerevisiae*. We observe that pairs of WGD paralogues in yeast are grossly over-represented as twins compared to pairs chosen at random from the network. In Section IV we conclude with a discussion of some implications of these results and give an outlook for future directions.

## II. DEFINITIONS, METHODS AND DATA

As is customary, we represent the connectivity of nodes in a graph  $\mathcal{G}$  in terms of an adjacency matrix  $\mathbf{A}$ . For undirected, unweighted networks, each element  $A_{ij} = A_{ji}$  is either 0 – if no link exists between node  $i$  and node  $j$  – or 1 otherwise. Assume that node  $i$  is contained within a connected, labeled subgraph  $\mathcal{H}$  of  $\mathcal{G}$ . The number of neighbors of  $i$  in  $\mathcal{H}$  is its subgraph degree  $k_i^{\mathcal{H}}$ . Two nodes  $i, j$  are twins in  $\mathcal{H}$  if they have identical neighbours in  $\mathcal{H}$ , *i.e.*

$$A_{il} = A_{jl} \quad \forall l \in \mathcal{H}, \quad l \neq i, l \neq j \quad . \quad (1)$$

One consequence of Eq. (1) is that  $i$  and  $j$  must have the same subgraph degree within  $\mathcal{H}$ , or  $k_i^{\mathcal{H}} = k_j^{\mathcal{H}}$ . To avoid the trivial case of twins with subgraph degree equal to one – which occurs when *e.g.* many nodes are connected to a hub – we require that  $k_i^{\mathcal{H}} = k_j^{\mathcal{H}} \geq 2$ . A pair of nodes  $i, j$  with subgraph degrees larger than two that satisfy Eq. (1) are type **A** twins if  $A_{ij} = 0$  and type **B** twins if  $A_{ij} = 1$ . Biologically the distinction between types **A** and **B** is motivated by the possibility that the ancestral protein of a paralogous pair was capable of homodimerization, *i.e.* it could interact with itself. Immediately after its duplication, the two paralogous proteins interact with each other and subsequent evolution can conserve this interaction. Type **B** twins with  $k^{\mathcal{H}} \geq 3$  are further denoted as type **B'** twins. These definitions are illustrated in Fig. 2 for an  $n = 5$  connected, labeled subgraph.

Using the graph animal algorithm, explained below, we obtain an estimate of the total number of connected, labeled  $n$  node subgraphs,  $\hat{H}_{ij}^{n, \mathbf{X}}$ , in which the pair  $i, j$  are type **X** twins, with  $\mathbf{X} = \mathbf{A}, \mathbf{B}$ , or  $\mathbf{B}'$ . We refer to  $\hat{H}_{ij}^{n, \mathbf{X}}$  as the type **X** twinning of the pair  $i, j$ . Furthermore, we refer to the pair  $i, j$  as type **X** twins if  $\hat{H}_{ij}^{n, \mathbf{X}} > 0$ , that is if  $i$  and  $j$  appear as type **X** twins in at least one connected, labeled  $n$  node subgraph in the network. Notice that a pair of nodes  $(i, j)$  cannot be both type **A** and type **B** twins, although the pair may appear as twins in one subgraph but

Source	Organism	$N$	$L$	$\langle k \rangle$
Butland <i>et al.</i>	<i>E. coli</i>	230	695	6.0
Krogan <i>et al.</i>	<i>S. cerevisiae</i>	2559	7031	5.5
Gavin <i>et al.</i>	<i>S. cerevisiae</i>	1374	6833	9.9
Batada <i>et al.</i>	<i>S. cerevisiae</i>	2752	9097	6.6

TABLE I: Global properties of the protein interaction networks studied. The quantity  $N$  is the number of nodes in the network,  $L$  is the number of links in the network, and  $\langle k \rangle$  is the average degree of a node in the network.

not in another. The total twinness for  $n$  node subgraphs in a network with  $N$  nodes is given by

$$\hat{T}_n^{\mathbf{X}} = \sum_{i,j}^N \hat{H}_{ij}^{n,\mathbf{X}}. \quad (2)$$

The carets in the above expressions denote quantities that are estimates based on a sampling method. We also define the twinness per subgraph,

$$\hat{t}_n^{\mathbf{X}} = \frac{\sum_{i,j}^N \hat{H}_{ij}^{n,\mathbf{X}}}{\hat{H}_n^N}, \quad (3)$$

to account for the dependence of twinness on the total number of connected, labeled  $n$  node subgraphs,  $\hat{H}_n^N$ , in the network. Twinness per subgraph enables comparisons between networks of different sizes and also between the original networks and their randomized counterparts.

The graph animal algorithm [9] makes it possible to obtain all of the estimates mentioned above. The algorithm, a generalization of Leath algorithms for lattice animals [16], grows connected subgraphs, and re-weights them to achieve uniform sampling of all labeled, connected subgraphs. Briefly, the graph animal algorithm proceeds as follows: (1) Pick a node at random from the network and mark it as ‘infected’; (2) Add each neighbour of that node in the network to the boundary list as ‘uninfected’; (3) While the number of nodes in the subgraph is less than  $n$  and the uninfected boundary list is not empty, do the following: Choose one uninfected boundary site and with probability  $p$  mark it as infected, join it to the subgraph, and update the boundary list with the neighbours of that node (which were not previously on the list) marked as uninfected. With probability  $(1 - p)$  mark the node as immune. Immune nodes can never be added to the subgraph. For more details see [9]. The graph animal algorithm enables uniform sampling of all labeled connected subgraphs of  $n$  nodes for a range of  $n$ .

Evaluating the statistical significance of the results requires a null model. We use the standard [17] (although in some cases inadequate [9]) null model based on link exchange or rewiring. Then the results for connected labeled subgraphs can be compared with the results for the same quantities in an ensemble of graphs with the same degree sequence. This also has the advantage of accommodating discrepancies in node degrees among different experimental constructions of the yeast PIN as indicated in Fig. 1. To construct this null model, one randomly selects two links,  $l_1$  and  $l_2$  where, say,  $l_1$  connects nodes  $a$  and  $b$  and  $l_2$  connects  $c$  and  $d$ . A link exchange move is performed and the resulting links now connect  $b$  to  $d$  and  $a$  to  $c$ . Exchanges that would result in multiple or self-links are rejected. This process is repeated many times, and any number of nominally independent realizations of the null hypothesis can be constructed by repeating link exchange moves.

In this study we analyze four recently constructed PINs, one for *E. coli* and three for *S. cerevisiae*. The *E. coli* network was made by Butland *et al.* using experimental data obtained from High-Throughput Tandem Affinity Purification (HT-TAP), followed by MALDI-TOF MS and LC-MS to identify the purified proteins. The first *S. cerevisiae* network was inferred by Krogan *et al.* using a machine learning algorithm that utilized the MIPS database of known stable complexes as the gold standard upon which the algorithm was trained. The raw experimental data for the Krogan *et al.* network was obtained using the same method as Butland *et al.* The second *S. cerevisiae* network was inferred by Gavin *et al.* using a logarithmically weighted superposition of the spoke and matrix methods of link inference. The raw experimental data was obtained by Gavin *et al.* using HT-TAP, followed by MALDI-TOF MS. Data for the third *S. cerevisiae* network was collected by Batada *et al.* through a comprehensive literature review of all known sources of Protein-Protein Interaction data. The network assembled by Batada *et al.* included only those interactions that were confirmed by several published sources, or were verified by a highly accurate method (such as Western Blot). The data for all these networks can be found in the on-line supplementary materials associated with Refs. [1, 2, 3, 18]. Table I summarizes various global properties of these networks, and their degree distributions are shown in Fig. 1.

The data set of Whole Genome Duplication (WGD) paralogues for *S. cerevisiae* was produced by Kellis *et al.* [12] and

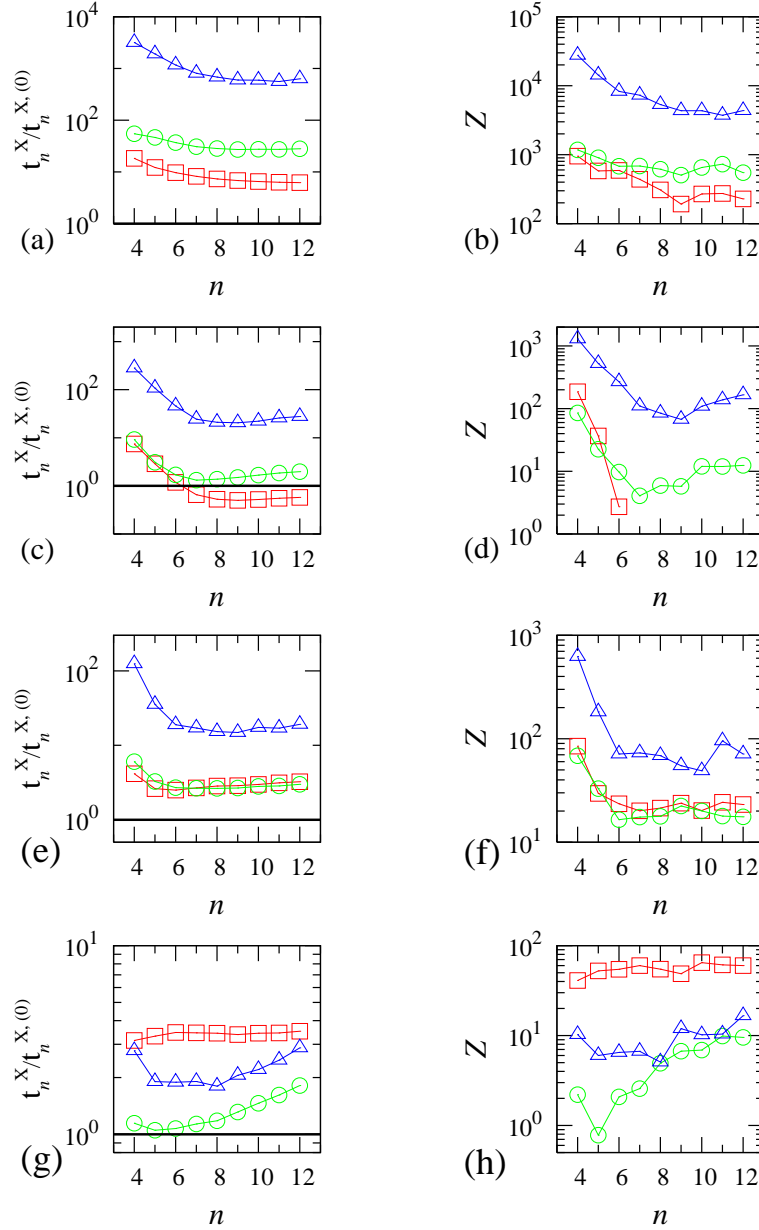


FIG. 3: Ratios of type **A**, **B** and **B'** twins per subgraph in the original PIN,  $\hat{t}_n^X$ , to twins per subgraph in the corresponding null model,  $\hat{t}_n^{X,(0)}$ , as a function of  $n$ , accompanied by  $Z$  scores for type **A**, **B** and **B'** twins per subgraph as a function of  $n$ . (a) and (b) are for the data set of Gavin *et al.*, (c) and (d) for Batada *et al.*, (e) and (f) for Krogan *et al.*, and (g) and (h) for the *E. coli* data set. Type **A** is represented by squares, type **B** by circles and type **B'** by triangles for each data set. All twin ratios, except type **A** in the Batada *et al.* data, are approximately independent of  $n$  at larger  $n$  and significantly over-abundant, with  $Z$  scores ranging up to  $\approx 10,000$ .

is found in the Supplementary Material of that publication. By sequencing and analyzing the genome of *Kluyveromyces waltii* – a related yeast species – these authors were able to identify paralogous genes resulting from a whole gene duplication event that occurred shortly after the two species diverged. The Kellis *et al.* data set was translated [14] so that it could be applied to the Krogan *et al.* data.

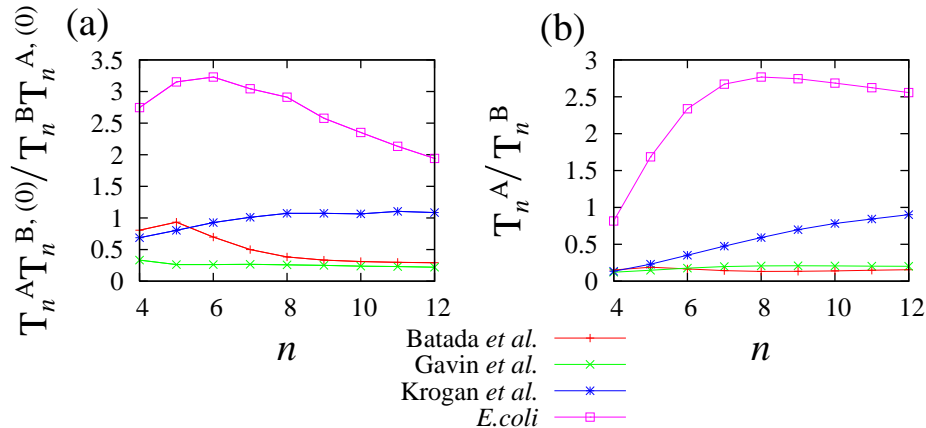


FIG. 4: (a) Ratio of type **A** total twinness to type **B** total twinness in a connected subgraph of size  $n$ , normalized by the average of the corresponding twinness for the randomized networks. (b) Ratio of type **A** total twinness to type **B** total twinness in connected subgraphs of size  $n$ . Error bars are not shown due to the fact that they would be smaller than the symbols. Errors include both the uncertainty associated with sampling and (for (a)) the variance in the values for the ensemble of randomized networks. Note that in both cases type **A** twins dominate for *E. coli* while type **B** twins dominate for *S. cerevisiae*.

### III. RESULTS

The first result of our analysis is a much higher twinness in the PINs than expected. As demonstrated in Fig. 3, in all cases twinness per subgraph is higher than in the null model – except for type **A** twins in the Batada *et al.* PIN. This is in stark contrast with the result obtained for twinness in the limit  $n \rightarrow N$ , where no twins of any type appear in either the original networks or in their randomized versions. In other words, considering the entire PIN, no two nodes of degree greater than two share all of their neighbours.

The statistical significance of the results for twinness is also demonstrated in Fig. 3, which shows the  $Z$  scores [26] for twinness per subgraph in the original PINs compared to their randomized counterparts. This data is also plotted on log-linear axes. Almost all  $Z$  scores in Fig. 3 are greater than 1, and some, particularly for type **B'** twins are several orders of magnitude larger. These extremely high  $Z$  scores indicate that rewired networks are not the optimal null model for PINs (see Refs. [7, 9].) Nevertheless the values obtained both for twin ratios and their corresponding  $Z$  scores are relatively stable for  $n \gtrsim 8$ . This indicates that a precise choice of  $n$  is not necessary.

The second result of our analysis is a statistically significant difference between the ratio of type **A** to type **B** twinness in *S. cerevisiae* PINs compared to the *E. coli* PIN. In Fig. 4b we see that the ratio of type **A** twinness to type **B** twinness is much higher for the *E. coli* PIN than for all three *S. cerevisiae* PINs. In Fig. 4a we normalize this ratio by the same ratio for the respective ensemble of randomized networks. This accounts for the differences in degree sequence among the yeast PINs. The difference between *E. coli* and *S. cerevisiae* persists after this normalization. It is particularly important that the Gavin *et al.* and Krogan *et al.* *S. cerevisiae* PINs are easily distinguished from the Butland *et al.* *E. coli* PIN because the experimental data for all three of these networks was obtained using the TAP-MS method. The systematic decline for *E. coli* in Fig. 4 might be a finite size effect. In fact, this PIN is an order of magnitude smaller than the *S. cerevisiae* PINs (see Table I).

Fig. 5 is a Zipf plot of twinness for each pair of nodes. We rank each pair  $i, j$  according to its twinness,  $\hat{H}_{i,j}^{n,\mathbf{X}}$ , and then plot this twinness value against its relative rank. Pairwise twinness and ranks for Fig. 5 were evaluated for  $n = 7$  node subgraphs. To facilitate the comparison of different PINs, we divide each pair's twinness by  $\hat{H}_7$ , the estimated total number of seven node subgraphs in the respective networks. Zipf plots for other  $n$ 's and data sets are qualitatively similar to those shown for the corresponding organism.

The difference between the prokaryote (*E. coli*) and the eukaryote (*S. cerevisiae*) PINs exhibited in Fig. 4 could be due to a higher number of type **A** twins than type **B** twins in *E. coli* – and the opposite in *S. cerevisiae*. Fig. 5 shows this is not the case, as for both the Krogan *et al.* *S. cerevisiae* PIN and the Butland *et al.* *E. coli* PIN the number of type **A** twins is roughly the same order of magnitude as the the number of type **B** twins. For *E. coli* the typical twinness of a type **A** twin is larger than the typical twinness of a type **B** twin, while the opposite is true for *S. cerevisiae*.

We now turn our attention to our third result, examining relationships between twinness and the evolutionary histories of PINs. Specifically, we focus on the set of paralogous proteins resulting from the whole genome duplication event in an ancestor of *S. cerevisiae* [12]. We started with the set of 457 WGD paralogous pairs identified by Kellis *et*

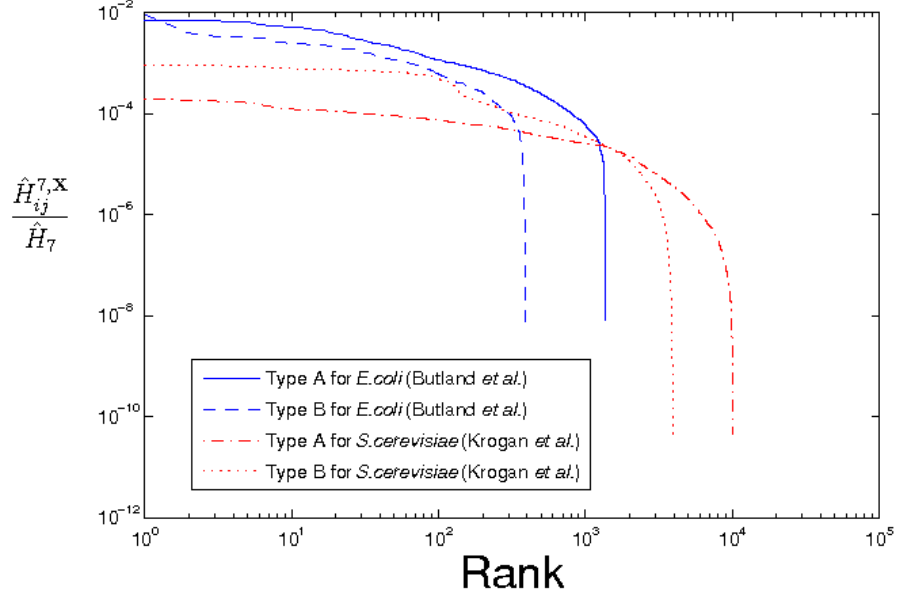


FIG. 5: Zipf plot for pairwise twinness in 7 node subgraphs. Each pair  $i, j$  is ranked according to its twinness,  $\hat{H}_{i,j}^{7,X}$ , and then plotted against its relative rank. Note that the frequencies for type **A** twins are greater than those for type **B** twins for *E. coli* while the opposite is the case for *S. cerevisiae*. The same trend is observed for the other two (Batada *et al.*, Gavin *et al.*) *S. cerevisiae* data sets, as well as other subgraph sizes.

*al.* [12]. We then searched for the WGD paralogues in the Krogan *et al.* *S. cerevisiae* PIN, and identified 117 WGD paralogues for which both member proteins were present in the PIN. The twinness of these 117 WGD paralogues was then measured, and a summary of this analysis is presented in Table II.

Our results indicate a strong correlation between WGD paralogous pairs and twins. We count the number of type **A**, **B**, and **B'** twins in the set of 117 paralogues and compared this to the same quantity averaged over many samples obtained by choosing 117 pairs at random from the PIN. The WGD paralogue set contains many more twins, of all types, than expected from a random set of node pairs. For type **A** we find 11 WGD paralogues that appear as twins, compared to an average of 0.36 for random samples of 117 pairs. Likewise for types **B** and **B'** we find 17 compared to 0.14 and 12 compared to 0.11, respectively. For all types the number of WGD paralogue twins is at least one order of magnitude greater than expected, and in the cases of **B** and **B'**, two orders of magnitude. In addition, WGD paralogues have a higher twinness (for all types) than pairs of 117 nodes chosen at random. However, when  $Z$  scores are calculated, this effect remains statistically significant only for type **B** and **B'**.

To guide the reader through Table II let us look at the case of type **A** twins for  $n = 5$  subgraphs. The entry of the first row indicates that 11 of the 117 WGD paralogues appear in at least one  $n = 5$  subgraph as type **A** twins, while the second row indicates that the number of type **A** twins expected in a sample of 117 randomly selected pairs is 0.36. The entry in the third row is the  $Z$  score for the total twinness,  $\hat{T}_5^A$ , summed only over the 117 WGD paralogues, compared to the total twinness of a random sample of 117 pairs. It should be noted that in the case of type **A** twins the  $Z$  score falls below 1 for large subgraphs in the Krogan *et al.* PIN. This is due to the fact that although there is large number of twins among the WGD paralogues ( $11 \gg 0.36$ ), their actual twinness values are low. From the results presented in Table II it is apparent that twinness (for type **B**) correlates strongly with WGD paralogues. This suggests that further refinements of our methods could result in a technique capable of identifying paralogous genes based on the network properties of PINs.

#### IV. DISCUSSION

Early interest in the topological structure of protein interaction networks (PINs) was driven in part by the observation of a scale-free degree distribution [5]. Since then various other topological properties of PINs have been studied, such as their disassortativity [17], clustering and over-abundance of small subgraphs or motifs [9]. Many of these structural properties have failed the test of robustness presented by newer higher confidence data [18, 19] – as also indicated in Fig. 1. Other properties that may be correlated with underlying biological criteria, such as protein

Type	Measure	$n = 5$	$n = 6$	$n = 7$	$n = 8$	$n = 9$	$n = 10$
<b>A</b>	Number of twins in set of WGD paralogous pairs.	11	11	11	11	11	11
	Same as above for an ensemble of random samples.	0.36	0.36	0.36	0.36	0.36	0.36
	$Z$ scores for total subgraphs in which paralogues appear as twins.	4.84	2.45	1.49	1.08	0.89	0.75
<b>B</b>	Number of twins in set of WGD paralogous pairs.	17	17	17	17	17	17
	Same as above for an ensemble of random samples.	0.14	0.14	0.14	0.14	0.14	0.14
	$Z$ scores for total subgraphs in which paralogues appear as twins.	30.72	22.85	19.04	17.25	17.42	17.68
<b>B'</b>	Number of twins in set of WGD paralogous pairs.	12	12	12	12	12	12
	Same as above for an ensemble of random samples.	0.11	0.11	0.11	0.11	0.11	0.11
	$Z$ scores for total subgraphs in which paralogues appear as twins.	25.22	30.96	27.53	23.92	21.49	20.89

TABLE II: Results for the set of 117 WGD paralogous pairs found in the *S. cerevisiae* PIN of Krogan *et al.* The first two rows for each type compare the number of twins found in the WGD paralogue set to the average number of twins expected when choosing 117 pairs at random from the network. WGD paralogues are twins  $\approx 100$  times more often than pairs chosen at random. The third row is the  $Z$  score for the total twinness of the paralogues, compared to the total twinness of an ensemble of sets of 117 randomly selected pairs of nodes. The  $Z$  scores establish the statistical significance of the observed correlation of WGD paralogues with type **B** twinness.

complexes [10], have proved to be more robust [2, 3], although some [11] have argued that protein complexes identified using clustering techniques on PINs lack biological significance.

In this paper we have proposed and studied a new structural property of networks that is not based on clustering algorithms or the identification of complexes – namely the occurrence of twin nodes in connected subgraphs. Our observation that PINs exhibit significantly higher twinness than randomized networks is robust for three different *S. cerevisiae* PINs despite the empirical disparity in the global characteristics of these networks. A further robust result is the marked difference between type **A** and type **B** twinness separating the *E. coli* PIN from all three *S. Cerevesiae* PINs studied. Based on the gross over-representation of WGD paralogues as type **B** twins, we propose that our measure is associated with the biological phenomenon of gene duplication.

To show that the PINs studied possessed statistically significantly higher twinness than expected, a null model was used. The extremely high  $Z$  scores observed in our analysis (see Fig. 3) makes it clear that this null model is not optimal for PINs. The commonly held picture of the global structure of a PIN is that it consists of a number of dense clusters of nodes, that are in turn loosely connected to each other. It is well documented that rewiring significantly reduces the frequency of dense subgraphs [7, 9]. Thus, due do the fact that rewiring destroys the characteristic dense clusters mentioned above, it is unlikely that a null model based on purely random rewiring is the best null model for these networks.

This specifically applies to our results in the following manner. A subgraph with many links will tend to have a large number of types **B** and **B'** twin pairs. (For instance, all pairs are twins in a complete graph.) However, in the rewired network, there are many fewer dense subgraphs and as such, many fewer types **B** and **B'** twin pairs are observed. As well the over-represented motifs of the networks we analyzed are known to be dense. These points offer a potential explanation for the high levels of types **B** and **B'** twinness observed. While this probably affects our first result (over-representation of twins in PINs), it could also affect our second result on the difference in levels of type **A** and type **B** twinness between *E. coli* and *S. cerevisiae* – as discussed below. However, the short comings of this null model could not impact our third result, the observed correlation between type **B** twinness and WGD paralogues.

The difference in the ratio of type **A** to type **B** twinness between the prokaryote *E. coli* and eukaryote *S. cerevisiae* could be explained if the *E. coli* network exhibited a fundamentally different type of clustering than the three *S. cerevisiae* networks. This is suggested by the results of [9], as the extended motifs of the *E. coli* network tend to be bipartite subgraphs (which contain many type **A** twins), while the extended motifs of the *S. cerevisiae* network are complete, or nearly complete subgraphs (which contain many type **B** twins). However, the connection between motifs and twins is not as trivial as it might first appear. Motifs are over-represented, but do not necessarily comprise the bulk of subgraphs. Another possible explanation for the ratio difference comes from biological considerations.



Consider a twin pair of proteins descended from the same ancestral protein capable of homodimerization. It would follow that the twin proteins would be candidates to be type **B** twins if the interaction arising from the homodimerization of the ancestral protein was conserved, where they would be candidates to be type **A** twins if that interaction was lost. Thus our results for the type **A** to type **B** twinness ratios in *E. coli* and *S. cerevisiae* could arise from a) a fundamental difference in the frequency of homodimerizing proteins between the two organism; b) differing rates of conservation of an ancestral homodimerization interaction between the two organisms or c) for reasons not related to homodimerization, such as different types of clustering. It is clear that to determine which of these cases is most likely a more sophisticated null model would be useful, particularly if it could reproduce the different types of clustering, and extended motifs found in the *E. coli* and *S. cerevisiae* PINs.

Turning our attention to our third result we note that paralogous pairs resulting from the whole genome duplication event in *S. cerevisiae* have been reported to be more likely to share at least one neighbour [14, 15]. While this is consistent with our result for twinness of WGD paralogues, no two nodes with degrees larger than two share all their neighbours. Our result is also consistent with the observation that WGD paralogues are separated by a shorter minimum-edge distance [14] and should thus appear in subgraphs of sizes that we have considered. Our analysis suggests that ancestral relationships between proteins can perhaps be uncovered using twinness in subgraphs, with the caveat that neither are all twins WGD paralogues, nor are all WGD paralogues twins. Furthermore it is possible that small scale duplicate proteins (such as those identified in [15]) will also appear as twins in the PIN. However, as discussed earlier, the high link density of motifs can be responsible for high twinness between nodes. Disentangling the effects of clusters from the effects of paralogous relationships is a subject for future work.

Moving on to directions not directly related to our results, we contend that analyses of connected subgraphs can shed light on the inference methods used to construct PINs. Recent TAP based experiments purify groups of proteins that are directly or indirectly bound to a bait protein. This protein group data is then converted into an interaction network using various inference methods [2, 3, 20]. Proteins that are purified as a group should lie close to each other in the inferred network, and thus be captured in our subgraphs. The criteria that were used to identify pairwise interactions from the protein group data should have a direct effect on the twinness of proteins. In fact, the gross differences between the PIN of Krogan *et al.* and that of Gavin *et al.*, both of which are based on TAP experiments, might be due to the different inference methods used [21]. We have not pursued questions related to inference methods in this work, but it does present a future direction of inquiry.

Finally, we point out that apart from biological motivations, twinness between nodes can also be used as a node similarity measure for other real-world networks. Node similarity based on the intersection of the neighbour sets has been used to study similarity between documents [22, 23], and has been extended to iterative definitions of similarity [24, 25]. The basic premise for these similarity measures, as for twinness, is that if the links between nodes are derived from their function, then the functional similarity between nodes can be inferred from the topological structure of the PIN. The method presented here is not iterative, but focuses on node similarity within local network structure, which is arguably of functional relevance.

- 
- [1] G. Butland, J.M. Peregrín-Alvarez, J. Li, W. Yang, X. Yang, V. Canadien, A. Starostine, D. Richards, B. Beattie, N. Krogan, M. Davey, J. Parkinson, J. Greenblatt, and A. Emili. *Nature*, 433 (2005) 531.
  - [2] N. J. Krogan *et al.* *Nature*, 440 (2006) 637.
  - [3] A. Gavin *et al.* *Nature*, 440 (2006) 631.
  - [4] R. Albert and A. L. Barabási. *Rev. Mod. Phys.* 74 (2002) 47.
  - [5] H. Jeong, S. P. Mason, A. L. Barabási, and Z. N. Oltvai. *Nature*, 411 (2001) 41.
  - [6] R. Milo, S. Shen-Orr, S. Itzkovitz, N. Kashtan, D. Chklovskii, and U. Alon. *Science*, 298 (2002) 824.
  - [7] M. E. J. Newman. *SIAM Review*, 45 (2003) 167.
  - [8] S. Wuchty, Z. N. Oltvai, and A-L. Barabási. *Nature Genetics*, 35 (2003) 176.
  - [9] K. Baskerville, P. Grassberger, and M. Paczuski. *q-bio/0702029* (2007).
  - [10] V. Spirin and L. A. Mirny. *PNAS*, 100(21) (2003) 12123.
  - [11] Z. Wang and J. Zhang. *PLOS Computational Biology*, 3:e107 (2007).
  - [12] M. Kellis, B. W. Birren, and E. S. Lander. *Nature*, 428 (2004) 617.
  - [13] A. Wagner. *Mol. Biol. Evol.* 18 (2001) 1283.
  - [14] G. Musso, Z. Shang, and A. Emili. *Trends in Genetics*, 23 (2007) 266.
  - [15] Y. Guan, M. J. Dunham, and O. G. Troyanskaya. *Genetics*, 175 (2007) 933.
  - [16] P. L. Leath. *Phys. Rev. B*, 14 (1976) 5046.
  - [17] K. Sneppen and S. Maslov. *Science*, 296 (2002) 910.
  - [18] N. N. Batada, T. Reguly, A. Breitkreutz, L. Boucher, B-J. Breitkreutz, L. D. Hurst, and M. Tyers. *PLOS Biology*, 4:e317 (2006).
  - [19] S. Coulomb, M. Bauer, D. Bernard, and M-C. Marsolier-Kergoat. *Proc. R. Soc. B*, 272 (2005) 1721.

- [20] G. D. Bader and C. W. V. Hogue. *Nature*, 20 (2002) 991.
- [21] J. Goll and P. Uetz. *Genome Biology*, 7 (2006) 223.
- [22] M. M. Kessler. *American Documentation*, 14 (1963) 10.
- [23] H. Small. *JASIST*, 24 (1973) 265.
- [24] G. Jeh and J. Widom. *KDD '02: Proceedings of the eighth ACM SIGKDD international conference on knowledge discovery and data mining*, (2002) 538.
- [25] E. A. Leicht, P. Holme, and M. E. J. Newman. *Phy. Rev. E*, 73 (2006) 026120.
- [26]  $Z$  score for a measurement  $x$  relative to an ensemble of null model measurements  $\{x^{(0)}\}$  is:  $Z = \frac{x - \langle x^{(0)} \rangle}{\sigma^{(0)}}$ , where  $\sigma^{(0)}$  is the standard deviation of  $x$  within the null ensemble.